IEEE Photonics Journal
An IEEE Photonics Society Publication

Blue Laser Diode System With an Enhanced Wavelength Tuning Range

Volume 12, Number 2, April 2020

Sani Mukhtar
Islam Ashry
Chao Shen
Tien K. Ng
Boon S. Ooi
M. Z. M. Khan

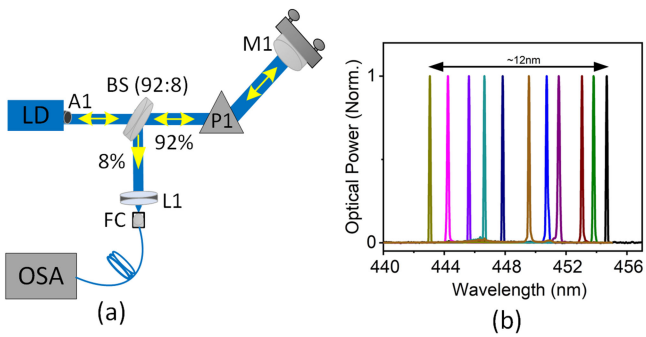

DOI: 10.1109/JPHOT.2020.2983448

Blue Laser Diode System With an Enhanced Wavelength Tuning Range

Sani Mukhtar,[1] **Islam Ashry**,[2] **Chao Shen**,[2] **Tien K. Ng**,[2] **Boon S. Ooi**,[2] **and M. Z. M. Khan** [1]

[1]Optoelectronics Research Laboratory, Electrical Engineering Department, King Fahd University of Petroleum and Minerals (KFUPM), Dhahran 31261, Saudi Arabia
[2]Photonics Laboratory, Computer, Electrical, and Mathematical Sciences and Engineering (CEMSE) Division, King Abdallah University of Science and Technology, Thuwal 23955-6900, Saudi Arabia

DOI:10.1109/JPHOT.2020.2983448

Manuscript received March 6, 2020; revised March 20, 2020; accepted April 16, 2020. Date of publication March 30, 2020 The work of SM and MZMK is supported by King Fahd University of Petroleum and Minerals through King Abdulaziz City for Science and Technology (KACST), Technology Innovation Center (TIC) for Solid-State Lighting (SSL) sub-awarded grant EE002381. The work of I. Ashry, C. Shen, T. K. Ng, and B. S. Ooi were supported by the King Abdullah University of Science and Technology (KAUST) through baseline funding BAS/1/1614-01-01 and KAUST-KFUPM special Initiative (KKI) program (REP/1/2878-01-01). The work of the authors were supported by the King Abdulaziz City for Science and Technology (KACST), Technology Innovation Center (TIC) for Solid-State Lighting primary grant KACST TIC R2-FP- 008 awarded to KAUST and the sub-awarded grant EE002381 to KFUPM. Corresponding author: M. Z. M. Khan (e-mail: zahedmk@kfupm.edu.sa).

Abstract: A prism-based self-injection locked seamlessly tunable blue InGaN/GaN laser diode composite cavity system is presented. A rigorous analysis of this external cavity diode laser (ECDL) system is performed at two different optical feedback powers. At 130 mA low injection, the high reflection system (HRS) exhibits a record wideband tuning span of $\sim$12.11 nm with a side-mode-suppression-ratio (SMSR) $\geq$ 15 dB, measuring as high as 40 dB, linewidth $\leq$110 pm, and a working power of about 3 mW. Whereas, a tuning range of 8 nm with linewidth $\leq$88 pm, SMSR $\geq$ 13 dB, reaching a maximum of 35 dB with 14.5 mW usable power is achieved from the low reflection system (LRS) at the same injection current. Moreover, an inverse relationship between the optical power and the tunability is observed in both the systems with a value as high as 180 mW exhibited by LRS configuration and attaining a tunability of 4.5 nm. Both systems highlight high stability even at higher injection currents and temperature. Such a robust, simple, and compact system may serve as a crucial light source in a plethora of diverse applications besides visible optical communications. To the best of our knowledge, this is the first report on a continuously tunable self-injection locked tunable laser system.

Index Terms: Tunable Laser, external cavity systems, self-injection locking.

1. Introduction

Tunable and narrow linewidth semiconductor laser diode systems in blue-violet region are indispensable sources in many applications; ranging from trace matter detection [1], biophotonics and bio-imaging [2], high resolution atomic and molecular spectroscopy [3], [4], holographic display and data storage [5], laser cooling [6], gas trace measurement [7], to sources for frequency conversion [8], and so on. Moreover, inherent features, such as simplicity, small footprint, cost-effective, and longer lifetime and efficiency, compared to their counterparts, for instance, metal-vapor, dye,

and gas lasers, make these diode lasers promising and competing sources in this multitude of applications. However, semiconductor laser diodes operating in the violet-blue-green wavelength region exhibit a broad lasing spectrum consisting of multiple longitudinal modes that inherently limit their potential deployment.

In a bid to address this shortcoming, two techniques have been widely explored in the literature to realize narrowband emission devices. Firstly, the monolithic approach employing grating structures in the form of distributed feedback (DFB) [9], [10], [11] and very recently, surface and sidewall DFB [12] gratings. These schemes demonstrated narrowband emission and are generally incorporated during the laser diode growth/fabrication process. Moreover, the realization of monolithic tunable laser with multi-section InGaN/GaN devices via altering selected section characteristics [9], [13] has also been reported in the green-blue region. However, monolithic integration of DFB gratings, as well as multi-section device fabrication on GaN, is still in the initial stage due to its sophisticated fabrication techniques and complexity, thus adding to increased device cost.

Conversely, the second approach relies on assisting techniques in ECDL configuration and may be considered as a post-growth/fabrication method. Besides providing narrowband emission, this system has unleashed the possibility to realize high performance visible tunable diode lasers. To this end, the well-known Litttrow and Littman-Metcalf ECDL configurations, which employ gratings as a wavelength-filtering element, had been successfully applied in the blue region of the electromagnetic spectrum with several demonstrations in the literature. In the following, we briefly review these tunable laser accomplishments concentrating on the blue region: A tunable ECDL system providing a $>$110 GHz long-mode-hop free tuning range, is demonstrated on 450 nm blue laser [14]. In 2014, Ruhnke *et al.* [15] reported a high power ECDL system with a narrow linewidth emission of $\sim$20 pm with a side-mode-suppression-ratio (SMSR) of 40 dB on 445 nm LD, and with a tuning span of $\sim$3 nm. Later, the effect of employing holographic and ruled feedback gratings on the ECDL tunability is investigated by Chi *et al.* [16]. A wavelength tuning range of $\sim$6.0 nm at $\sim$450 nm, with a spectral linewidth and SMSR of $\sim$20 pm and $>$20 dB, respectively, is demonstrated while achieving $\sim$80 mW usable power. In the following year, Ding *et al.* [17] successfully extended the tuning range to 7.2 nm by employing a high power blue LD in Littrow ECDL configuration, with a linewidth of $\sim$100 pm and SMSR of up to $\sim$35 dB. Subsequently, they further studied the influence of various grating parameters on the performance of an ECDL system and demonstrated a tuning window of $\sim$10.9 nm (439.5–450.4 nm) at threshold current and 8.3 nm (442.2–450.5 nm) at 300 mA, with an SMSR of 10–20 dB [18]. Besides wavelength tunability, the possibility of attaining very narrow linewidth emission (single longitudinal mode, SLM, emission) from the ECDL system is reported by Chen *et al.* [19] at 445 nm with a value of 4.7 MHz, while also demonstrating a wavelength tuning window of 4.3 nm with an output power of 20 mW.

Very recently, an alternate ECDL system with wavelength filter-less element, by incorporating only a partial reflector, was proposed and demonstrated by our group on green LD emitting at $\sim$530 nm [20]. The system relies on self-injection locking to lock a particular wavelength mode [21], [22], thereby exhibiting a significant reduction in the optical linewidth, below 100 pm, and SMSR $>$10 dB, compared to the free-running (FR) laser case. Moreover, a tunability of $\sim$7.1 nm is also achieved by merely varying the external cavity length. Such a simple configuration negates the well-known limitations of Litttrow and Littman-Metcalf ECDL systems, such as bulky and complex nature, susceptibility to misalignment, high cost, instability at higher injection current, etc. [23]–[26]. Hence, the self-injection locked ECDL system is a promising tunable laser source for practical applications, thanks to its niche features such as cost-effectiveness, stability, besides simplicity.

In this work, we report on a novel prism-based tunable self-injection locked blue ECDL system and demonstrate a record wavelength tunability of 12.11 nm ($\sim$442.69–454.8 nm) while significantly improving the system performance. Thanks to the integrated prism between the reflecting mirror and the front facet of the commercially available InGaN/GaN blue laser diode, which enables the achievement of seamless tunability while maintaining an optical linewidth $\leq$110 pm and SMSR $>$15 dB throughout the wavelength window. These performance characteristics, to our knowledge, are the finest-reported values in the blue region. Furthermore, two ECDL systems with different feedback optical powers are comprehensively investigated in terms of temperature, injection

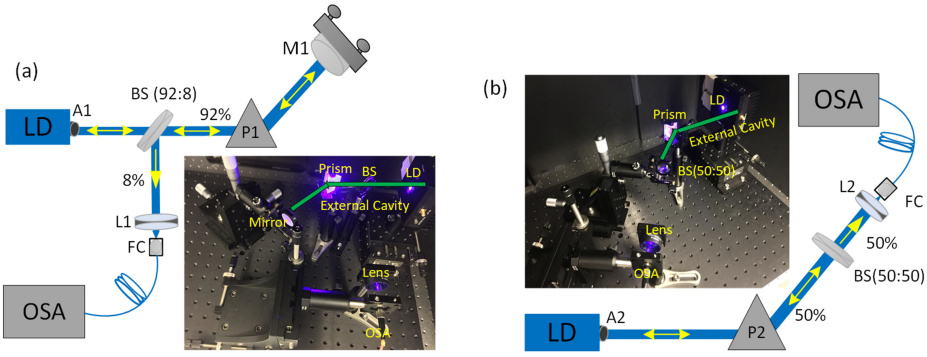

Fig. 1. Block diagram of (a) high reflection (HRS) and (b) low reflection (LRS) self-injection locked tunable blue laser system. The respective insets show the photograph of the laboratory setup.

current, and external cavity length. While the high reflection system (HRS) exhibit the above high-quality performance characteristics, a tuning span of 8 nm (∼443–451 nm) with a linewidth of $<$85 pm and SMSR $>$13 dB is achieved from the low reflection system (LRS) configuration, with both systems exhibiting high stability at elevated injection currents and temperatures.

2. Experimental Setup

The block diagrams of the reported systems are shown in Figs. 1(a) and (b) along with their respective laboratory photographs in the insets. In the case of HRS, shown in Fig. 1(a), a pellicle beam splitter, BS1, 92:8% (Thorlabs, BP107) is employed to extract the 8% usable optical power from the system. A high power TO-can blue Fabry Perot (FP) laser diode (LD), emitting at ∼450 nm (SN-LD-P06, SaNoor Technologies), is installed on a temperature-controlled mount (Thorlabs, TCLDM9) and the laser beam is collimated with an aspheric lens (Thorlabs, A110TM-A) A1, as shown in Fig. 1(a). The 92% of the laser optical power is passed through an equilateral dispersive prism P1 (Thorlabs, PS858) towards a highly reflective mirror M1 (Thorlabs, PF10-03-P01, with 97.5% reflection), which is placed on a kinematic mount (Thorlabs, KM100), installed on a translation stage, and serves as the first facet of the external cavity. The laser beam, after reflecting from M1, is then feedback into the laser active region via the prism and the front facet of the LD, which also serves as the other reflector of the external cavity. The knobs of the kinematic mount are utilized to tune the external cavity length for self-injection locking (SIL) as well as the wavelength tuning. The 8% usable optical power of the system is then coupled into an optical fiber via a plano-convex lens (Thorlabs, LA-1951-A) L1 while the other fiber end is connected to an optical spectrum analyzer (Yokogawa, AQ6373B, 20 pm resolution) via a fiber connector (FC) for diagnostic purpose.

On the other hand, the LRS illustrated in Fig. 1(b), employs a 50:50% beam splitter BS2 (Thorlabs, BSW27), serving as a partial mirror, and is placed on the kinematic mount of Fig. 1(a) in place of M1. The 50% usable optical power, in this case, is collected from the other end of BS2 and then coupled to an optical fiber via a plano-convex lens L2 for diagnostic purposes. The reflected 50% of the laser power from BS2 is then feedback into the laser active region via the prism, aspheric lens A2, and the front facet of the LD in a similar manner as that of HRS of Fig. 1(a). It is noteworthy to mention at this point that HRS (LRS) system exhibits high (low) injection ratio R (i.e., the ratio of the LD FR power to the feedback power) since 92 (50)% of the laser power is feedback into the system and 8 (50)% exiting out as a usable power.

3. Results and Discussions

L-I-V characteristics of the FR ∼450 nm blue FP laser diode are measured at room temperature (20 °C) and are shown in Fig. 2(a) wherein a threshold current (I_{th}) of about 124 mA is apparent.

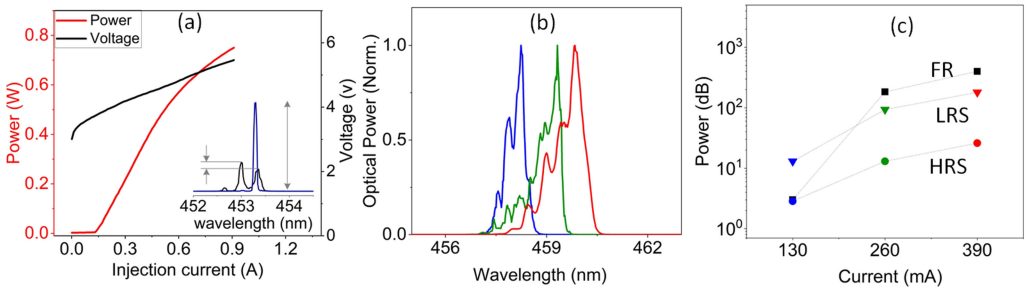

Fig. 2. Free-running ~450 nm blue LD performance at 20 °C room temperature. (a) L-I-V characteristics and (b) lasing spectrum at low (130 mA, blue), medium (260 mA, green), and high (390 mA, red) injection currents. (c) Measured usable power at low (blue), medium (green) and high (red) injection currents for both HRS (closed circles) and LRS (closed inverted triangles) configurations alongside the FR LD optical power (black closed squares). The inset of (a) shows the comparison between the FR (black) and the locked (blue) spectrums, where the respective arrows depicts the exhibited SMSR. A substantial increase in SMSR is observed in the case of locked mode spectrum.

This high power laser diode exhibit a near-threshold slope efficiency of ~0.9 W/A. Fig. 2(b) plots the corresponding FR lasing spectrum at low (130 mA), medium (260 mA), and high (390 mA) injection currents showing an apparent multi-longitudinal mode behavior with a broad 3 dB bandwidth of 650, 760 and 850 pm, respectively. The measured optical power at the front facet of the laser mount at these injection currents is briefed in Fig. 2(c), with measured values of 3.4, 183, and 400 mW, respectively. These are the injection currents selected for the analysis of the HRS and LRS tunable configurations at two different temperatures, 20 and 40 °C, as well as two external cavity lengths of 16 and 22 cm. Moreover, unlike the deployment of wavelength filtering elements in other ECDL systems, here, we exploit the SIL assisting scheme to lock a particular longitudinal mode of the two-cavity system (laser cavity 'L' and the external cavity 'L_E'). Later, we achieved seamless wavelength tunability with a step size dictated by LD mode spacing (~50 pm) by carefully tuning the external cavity length.

To understand the SIL phenomenon qualitatively, consider the following gain and phase condition relations under optical injection [27]:

$$\Delta g = g_{inj} - g_{th} = -L^{-1}\kappa \cos \phi_{inj} \tag{1}$$

$$\Delta\phi_L = \phi_L - \phi_{th} + \kappa\sqrt{(1+\alpha^2)}\sin\left(\phi_{inj} + \tan^{-1}\alpha\right) \tag{2}$$

where $g_{th}(g_{inj})$ is the LD gain threshold under FR (optical feedback), $\kappa = 2|C|\sqrt{R}$ is the optical injection coefficient with a coupling efficiency C, $\phi_{th}(\phi_L)$ is the phase of a particular LD longitudinal mode in FR (under optical feedback) and ϕ_{inj} is the feedback phase of the external cavity mode, α is the linewidth enhancement factor of the LD that is related to the dependence of the active region refractive index on the gain change. Under locking condition, negative Δg is attained while $\Delta\phi_L = 0$, suggesting a reduced threshold gain of the LD under locking, thereby reducing the threshold current. Moreover, the selected LD mode would be resonant in the two-cavity system, thus surviving by consolidating the optical power of the system while suppressing the other adjacent modes, and improving both the optical linewidth (measured at the full width at half maximum) and the SMSR. This would significantly reduce system noise. Moreover, by carefully tuning the external cavity length ϕ_{inj} could be altered in such a manner to satisfy the phase condition for the next longitudinal wavelength mode of the LD, thereby attaining seamless wavelength tuning of the system.

3.1 Effect of Injection Current

Fig. 3 shows the room temperature tunability results of the reported self-injection locked HRS and LRS configurations at a fixed 22 cm external cavity length for three different injection currents

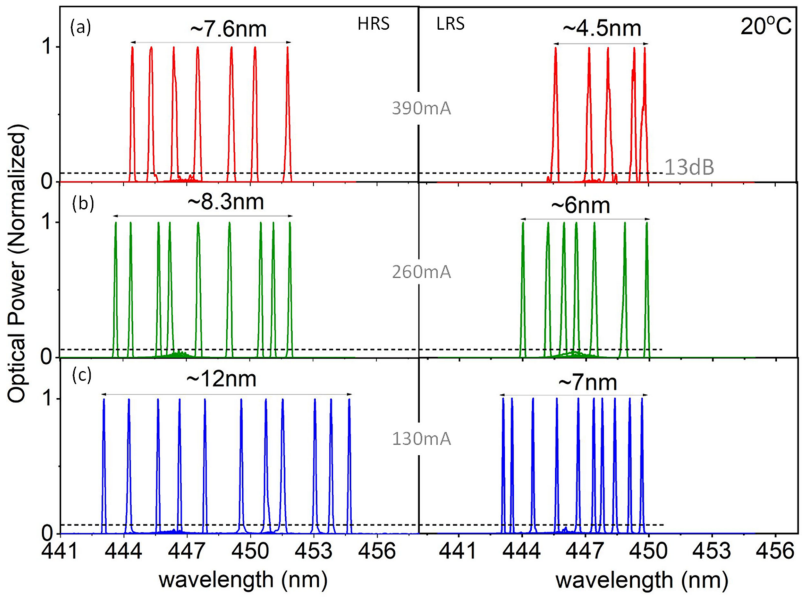

Fig. 3. The superimposed lasing spectrum of the HRS and LRS configurations at 20 °C room temperature, showing the wavelength tuning range of the system at (a) low (130 mA), (b) medium (260 mA), and (c) high (390 mA) injection currents. The external cavity length is 22 cm.

above the threshold, *viz.* low, medium and high currents. Both configurations exhibit a similar trend of wideband tuning window at low injection current while the value dropped with increasing current injection. For instance, a tunability of 12.0 (7.0) nm is measured at 130 mA while it decreases to 8.3 (6.0) nm at 260 mA and eventually to 7.6 (4.5) nm at 390 mA, for the HRS (LRS) configuration. This is attributed to the difficulty in SIL of the LD modes due to increased mode competition across them since several of them would attain the lasing condition at high injection current and appears in the emission spectrum. Moreover, an increase in α –factor at high injection may also increase the number of densely spaced external cavity mode ($\sim$0.5 pm spacing) solutions of Eq. (2) for these sparsely spaced LD modes, thus making SIL even more difficult with inferior efficiency. Nevertheless, this observed inverse relationship of tuning window with injection current is similar to that of Littrow based ECDL systems reported in the literature [17], [18], [20]. Furthermore, smooth, progressive discrete wavelength tunability across the tuning window is demonstrated by both the configuration and at any injection current. Thanks to the inclusion of the prism in our system, which assisted in the effortless tuning of the external cavity by slightly dispersing the reflected power into the LD and hence achieving efficient selection and locking of LD modes.

On comparing the tunability across HRS and LRS configurations, a considerable reduction in the wavelength tunability in the range of $\sim$2.3–5.0 nm is noted in the latter case, at different injection currents, as depicted in Fig. 3. We postulate that the variation in the feedback power into the LD of these systems, and hence corresponding different estimated R of ~ -0.7 and ~ -3.0 dB, are accountable for this performance variation. Increased feedback power into the LD in the HRS configuration ensures high R of the system and hence exhibiting large κ values and comparatively increased number of solutions to Eq. (2). In other words, more external cavity modes would be available to satisfy the phase condition for a particular LD mode to sustain in the two-cavity system while reducing g_{inj} considerably, as dictated by Eq. (1). This probably enabled exploiting the complete gain-bandwidth of the LD at a fixed injection current with relatively constant α –factor, thereby significantly enhancing the tunability of HRS compared to the LRS configuration.

In terms of system efficiency, Fig. 2(c) compares the measured working power of both the systems alongside the FR LD power. At low (130 mA) injection current, HRS and LRS SIL based

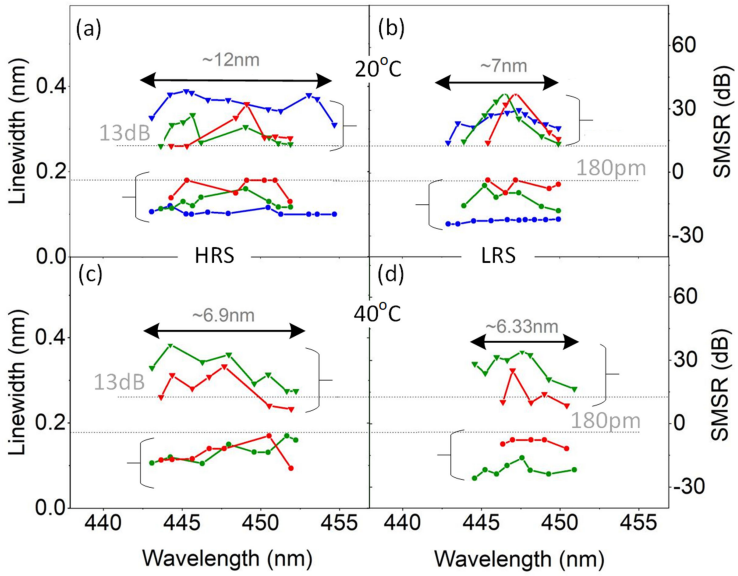

Fig. 4. Performance evaluation of HRS (a) and (c) and LRS (b) and (d) configurations at (a) and (b) 22 cm, and (c) and (d) 16 cm external cavity length, in terms of optical linewidth (circles) and, SMSR (inverted triangles). The blue, green, and red markers correspond to 130, 260, and 390 mA injection currents, respectively. All the measurements are performed at 20 °C room temperature.

ECDL configurations demonstrate a usable power of ∼3 and ∼14 mW, respectively, compared to the FR LD case of ∼3.4 mW that is measured at the LD front facet. On the other hand, if the unlocked FR LD power (i.e., without locking) is measured at the corresponding outputs of both the configuration *viz.* HRS (at 8% of BS1) and LRS (at 50% of BS2), the values are ∼0.2 and ∼2.3 mW, respectively. Comparing these unlocked FR LD power values with that of the SIL HRS and LRS ECDL system configurations, a significantly increased usable power is exhibited by the latter cases, thus indicating high system efficiency at low injection current. This is a strong signature of SIL wherein the gain threshold (g_{inj}), and hence the threshold injection current of the LD is reduced, as pointed out by Eq. (1). At medium and high injection currents, as expected, HRS and LRS configurations exhibited working powers of ∼8 and ∼50% of the FR LD front-facet power. This translates to corresponding 13 (23) and 93 (180) mW at 260 (390) mA. Furthermore, should the output power is collected from the rear facet of the LD, which was inaccessible in this work, this would significantly improve the working powers of both the SIL systems, reaching close to ∼70–80% of the FR LD front facet power should an as-cleaved facet reflectivity of ∼20–30% is considered.

The room temperature characteristics of each locked mode within the tuning window are evaluated in terms of SMSR and optical linewidth and are summarized in Figs. 4(a) and (b) for the HRS and LRS configurations, respectively. A general observation could be deduced by observing these figures; at low injection, the performance of HRS and LRS configurations are found to be superior and more consistent across the tuning range compared to the medium and high injection current operation. In this case, a linewidth (SMSR) reaching values of ∼100–110 pm (∼23–40 dB) and ∼77–88 pm (15–30 dB), with average values of ∼105 pm (31.5 dB) and ∼83 pm (22 dB), respectively, are noted. It is to be noted that achieving these performance parameters with an integrated high power LD in the SIL based system is non-trivial since injection locking efficiency degrades at high power and injection current operations. Nevertheless, these values are considerably superior to other low power SIL based [18], [19] and comparable to high-power Littrow based tunable systems. This substantiates the efficacy of our cost-effective and straightforward system compared to other bulky and costly ECDL systems reported in the literature. Moreover,

the fluctuation in SMSR and linewidth of both the configurations could be further minimized by improving the locking efficiency by fine-tuning of external cavity length with piezo-motorized stages. It is noteworthy to mention that the demonstrated tunability of 12 nm is the largest value reported in the literature, to the authors' knowledge, besides exhibiting these high-performance characteristics. Furthermore, we set threshold limits of $\leq$110 pm ($\geq$15 dB) of the optical linewidth (SMSR) for the low current injection case while $\leq$180 pm ($\geq$13 dB) for the other injections, at room temperature, to evaluate our tunable system performance. Hence, the experimentally reported tuning window in this work is smaller than actually observed values. Referring back to Figs. 4(a) and (b), at medium and high injection currents, a comparatively broader mean optical linewidth noticed from both the systems while maintaining high SMSR. As such, a linewidth (SMSR) of $\sim$100–180 pm ($\sim$13–35 dB) and $\sim$100–170 pm ($\sim$13–38 dB) with mean values $\sim$140 pm ($\sim$24 dB) and $\sim$135 pm ($\sim$25 dB) are observed from HRS and LRS configurations, respectively, at $>$ 130 mA. We postulate that the slightly dispersed feedback light into the laser active region may facilitate simultaneous locking of adjacent LD modes that are competing. This is highly probable since a large number of external cavity mode solutions exist for a particular LD mode at high injections. Moreover, the various non-linear phenomena are prone to occur at high injection currents and temperatures that may again render the locking difficult and hence reduce the system tunability as well as performance. Nevertheless, a significantly improved average SMSR value by $\sim$6.0 dB is observed from both the configurations when compared to other SIL based ECDL systems in literature [18] and is similar to the SMSRs reported from grating filter based ECDL systems [14]–[16]. Thanks to the inclusion of prism that assisted in significantly improving the performance while preserving the simplicity and robustness of the system, which are crucial in the practical deployment of ECDL systems.

3.2 Effect of External Cavity Length

Changing the external cavity length alters the performance of the SIL based ECDL system, as has been observed in the literature [20]. To investigate this effect, we reduced the external cavity length to 16 cm, by decreasing the distance between the mirror and the prism, and evaluated the system performance at both low and high injection currents at room temperature. The results, which are summarized in Figs. 4(c) and (d), display minor reduction in the tuning window to 11.5 nm for the HRS and 6.4 nm for LRS configurations, at 130 mA, while exhibiting corresponding measured linewidth (SMSR) of 90–109 pm (19–37 dB) and 61–86 pm (13–35 dB), on decreasing the external cavity length from 22 to 16 cm. Moreover, as observed in the longer external cavity case, a decrease in tuning window to 8.2 (6.0) at 260 mA and finally to 7.6 (5.1) nm at 390 mA for the HRS (LRS) configuration is noted. Nevertheless, within the set threshold, the measured optical linewidth and the SMSR of the short cavity system are observed to be similar to that of the long cavity system even at $>$130 mA. This is contrary to the other works reported in the literature where both linewidth and SMSR degrade with shorter external cavity length, and so is the tuning window [20]. We attribute this performance preservation with a minimal drop in the tuning window to the inclusion of the prism in the external cavity that facilitated better locking efficiency. Furthermore, in terms of modulation bandwidth improvement, both external cavity length SIL systems are expected to exhibit superior performance than the FR case, as has been observed in literature, with the shorter cavity lengths being better than the longer cavity length [21]. It is also worth mentioning at this instant that if the external cavity length is considered as a tuning parameter of the system, besides injection current, then an overall wavelength tuning window of $\sim$12.11 nm and $\sim$8.0 nm are demonstrated by the HRS and LRS configurations, respectively.

3.3 Effect of Temperature

The influence of temperature on the performance of both the system is depicted in Fig. 5 considering the thresholds of $\leq$180 pm optical linewidth and $\geq$10 dB SMSR, and at 260 and 390 mA injection currents. A general observation of redshift in the tuning span is noted with increasing temperature for both the system configurations at different external cavity lengths and injection currents. This

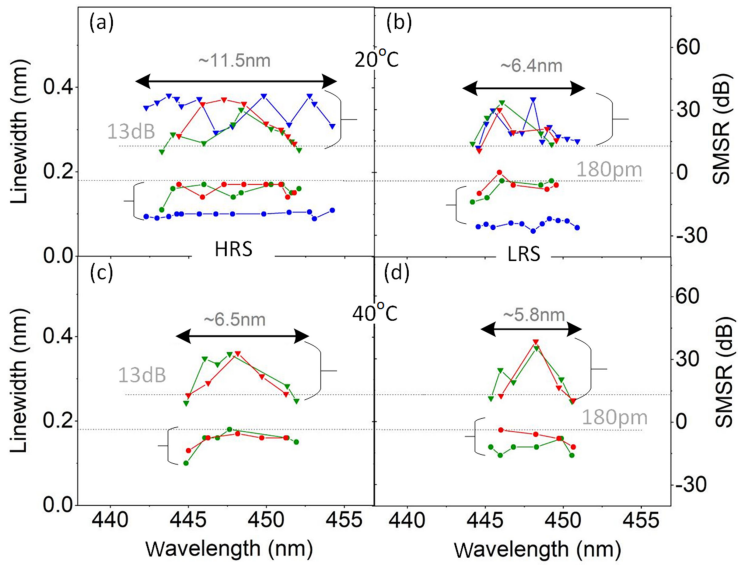

Fig. 5. Performance evaluation of HRS (a) and (c) and LRS (b) and (d) configurations at (a) and (b) 22 cm, and (c) and (d) 16 cm external cavity length, in terms of optical linewidth (circles) and, SMSR (inverted triangles). The green and red markers correspond to 260 and 390 mA injection currents, respectively. All the measurements are performed at 40 °C.

is indicative of the temperature-dependent quantum-well transition energy shrinkage leading to the redshift of the LD active-region gain profile. Moreover, associated with the redshift is shrinking of tuning window with temperature rise. For instance, at 22 cm cavity length, a tuning window of 8.3 nm at 20 °C decreases to 6.9 nm at 40 °C for the HRS configuration at 260 mA, with a similar trend at high injection current. Moreover, shortening the external cavity length from 22 to 16 cm at 40 °C further reduces the tuning widow to 6.5 nm. A similar wavelength tuning behavior is also exhibited by the LRS configuration at high temperature, as illustrated in Fig. 5(b) and (d). We ascribe these observations to further intense mode competition and hence the difficulty in locking the mode in the two-cavity system that exhibits elevated non-linear dynamics as well as mode solutions to Eq. (2) due to the temperature rise (increased α–factor). Nevertheless, the inclusion of prism has assisted in achieving adequate SIL condition at elevated temperatures and injection currents and hence improving the system stability. This could further be inferred from Fig. 5 wherein both HRS and LRS configuration exhibit analogous linewidth (SMSR) characteristics at high temperature compared to room temperature scenario with the extracted value of ∼95–170 pm (∼10–38 dB) and ∼70–160 pm (∼10–35 dB), respectively, considering both injection currents. Moreover, the corresponding mean values are found to be ∼130 pm (∼24 dB) and ∼115 pm (∼22 dB) within the respective wavelength tuning windows. This suggests that the performances of both the systems at high injection currents and temperatures, in the high-power systems, are preserved, unlike in other low-power SIL tunable laser systems where performance degradation is noted [20].

3.4 System Stability

To assess the stability of the proposed HRS and LRS configurations, a 30 minutes performance analysis with three minutes' interval is conducted on both the external cavity lengths. In each case, the injection current and temperature are fixed at 130 mA and 20 °C, respectively. While for the 22 cm cavity, the chosen mode peak wavelength is 447.5 nm, for the shorter 16 cm cavity length, 445.25 nm mode is selected for the analysis. The monitored results of the optical linewidth, SMSR, integrated, and peak optical power of the mode are plotted in Fig. 6 and 7. It is worth mentioning here that the peak wavelengths of both the systems (not shown) are found

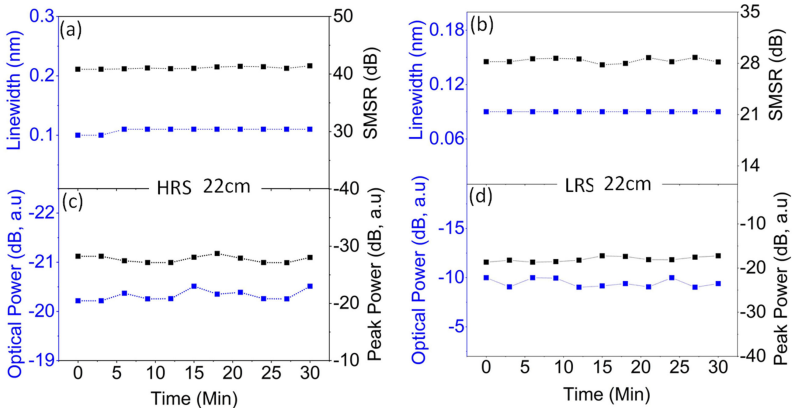

Fig. 6. Stability of both the HRS and the LRS configurations at 22 cm external cavity length and observed for 30 minutes. (a) and (b), optical linewidth and SMSR, and (c) and (d), integrated, and peak optical power.

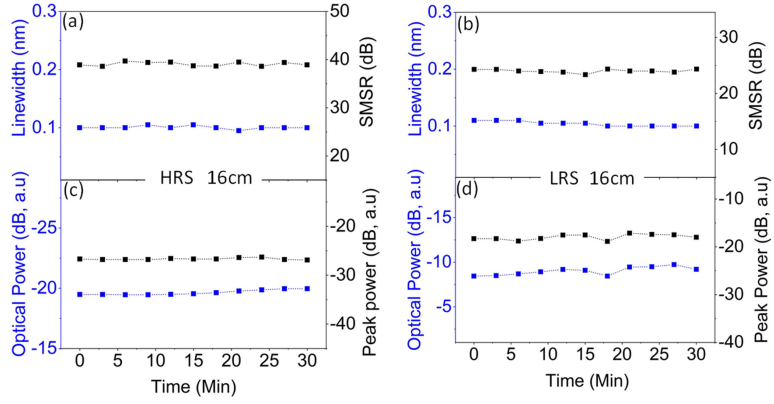

Fig. 7. Stability of both the HRS and LRS configurations at 16 cm external cavity length and observed for 30 minutes. (a) and (b), optical linewidth and SMSR, and (c) and (d), integrated, and peak optical power.

to be very stable, with a minor fluctuation of $\pm$5 pm throughout the monitoring window. Both the system demonstrated excellent stability with 22 cm cavity length with linewidth and SMSR variation of $\pm$3 pm and $\pm$0.3 dB, respectively. Whereas, a slight change in the integrated and peak power is observed within the monitoring window with an exhibited variation of $\pm$0.3 and $\pm$0.4 dB, respectively. Nevertheless, these variations are comparable to the other SIL based ECDL system. Furthermore, referring to Fig. 7, which plots the stability performance of 16 cm cavity, variations of $\pm$1.5 pm, $\pm$0.25 dB, $\pm$0.4 and $\pm$0.5 dB in the linewidth, SMSR, integrated and peak powers are observed from both the systems. We attribute this unusual high stability from shorter cavity length possibly to the incorporation of prism in the system, as has been discussed above. This demonstrates the robustness of our prism-based HRS and LRS configurations that are a promising source of practical deployability in a multitude of applications.

4. Conclusion

In summary, a continuously tunable 450 nm blue InGaN/GaN laser diode external cavity system incorporating a prism and self-injection locking scheme is proposed and demonstrated. A significant enhancement in the wavelength-tuning window of up to 12.11 and 8 nm with $\sim$3 and 14.5 mW

working powers was achieved via HRS and LRS configuration at just above threshold current, with optical linewidth $\leq$110 pm and SMSR $\geq$ 15 dB and reaching as high as 40 dB. Additionally, the maximum optical power of 180 mW at 390 mA injection current is exhibited by the LRS system with a tuning window of 4.5 nm. In general, both the systems are found to be very stable and have the potential to be deployed as a tunable source in the multidisciplinary field of applications owing to its robustness, simplicity, and cost-effective features.

References

[1] K. Hdlc *et al.*, "Blue laser diodes for trace matter detection," *Opt. Appl.*, vol. 40, no. 3, pp. 641–651, 2010.
[2] A. Müller *et al.*, "Diode laser based light sources for biomedical applications," *Laser Photon. Rev.*, vol. 7, no. 5, pp. 605–627, 2013.
[3] M. Chi, O. B. Jensen, A. K. Hansen, and P. M. Petersen, "Tunable high-power external-cavity GaN diode laser systems in the visible spectral range," in *Laser Technology and Its Applications*, Yufei Ma, Ed., London, UK: IntechOpen Limited, 2019, ch. 1, pp. 3–21.
[4] I. S. Burns, J. Hult, and C. F. Kaminski, "Spectroscopic use of a novel blue diode laser in a wavelength region around 450 nm," *Appl. Phys. B Lasers Opt.*, vol. 79, no. 4, pp. 491–495, 2004.
[5] T. Tanaka *et al.*, "Littrow-type external-cavity blue laser for holographic data storage," *Appl. Opt.*, vol. 46, no. 17, pp. 3583–3592, 2007.
[6] Y. Shimada *et al.*, "A simplified 461-nm laser system using blue laser diodes and a hollow cathode lamp for laser cooling of Sr," *Rev. Sci. Instrum.*, vol. 84, no. 6, 2013, Art. no. 063101.
[7] C. Dyroff, "Tunable diode-laser absorption spectroscopy for trace-gas measurements with high sensitivity and low drift," *Karlsruhe Ser. Photon. Commun.*, vol. 5, pp. 35–54, 2008.
[8] N. Ruhnke *et al.*, "Single-pass UV generation at 2225 nm based on high-power GaN external cavity diode laser," *Opt. Lett.*, vol. 40, no. 9, pp. 2127–2129, 2015.
[9] J. A. Holguín-Lerma, T. K. Ng, and B. S. Ooi, "Narrow-line InGaN/GaN green laser diode with high-order distributed-feedback surface grating," *Appl. Phys. Express*, vol. 12, no. 4, 2019, Art. no. 042007.
[10] J. H. Kang *et al.*, "DFB laser diodes based on GaN using 10th order laterally coupled surface gratings," *IEEE Photon. Technol. Lett.*, vol. 30, no. 3, pp. 231–234, Feb. 2018.
[11] D. Hofstetter, R. L. Thornton, L. T. Romano, D. P. Bour, M. Kneissl, and R. M. Donaldson, "Room-temperature pulsed operation of an electrically injected InGaN/GaN multi-quantum well distributed feedback laser," *Appl. Phys. Lett.*, vol. 73, no. 15, pp. 2158–2160, 1998.
[12] Z. Deng, J. Li, M. Liao, W. Xie, and S. Luo, "InGaN/GaN distributed feedback laser diodes with surface gratings and sidewall gratings," *Micromachines*, vol. 10, no. 10, pp. 1–10, 2019.
[13] C. Shen *et al.*, "High-modulation-efficiency, integrated waveguide modulator-laser diode at 448 nm," *ACS Photon.*, vol. 3, 2, pp. 262–268, 2016.
[14] J. Hult, I. S. Burns, and C. F. Kaminski, "New light sources–Wide tuning range and rapid scanning blue extended cavity diode lasers," in *Proc. Optics InfoBase Conference Papers*, 2006, Paper ThB1.
[15] N. Ruhnke *et al.*, "400 mW external cavity diode laser with narrowband emission at 445 nm," *Opt. Lett.*, vol. 39, no. 13, pp. 3794–3797, 2014.
[16] M. Chi, O. B. Jensen, and P. M. Petersen, "Tuning range and output power optimization of an external-cavity GaN diode laser at 455 nm," *Appl. Opt.*, vol. 55, no. 9, pp. 2263–2269, 2016.
[17] D. Ding, X. Lv, X. Chen, F. Wang, J. Zhang, and K. Che, "Tunable high-power blue external cavity semiconductor laser," *Opt. Laser Technol.*, vol. 94, pp. 1–5, 2017.
[18] D. Ding *et al.*, "Influence of grating parameters on the performance of a high-power blue external-cavity semiconductor laser," *Appl. Opt.*, vol. 57, no. 7, pp. 1589–1593, 2018.
[19] M. H. Chen, S. C. Hsiao, K. T. Shen, C. C. Tsai, and H. C. Chui, "Single longitudinal mode external cavity blue InGaN diode laser," *Opt. Laser Technol.*, vol. 116, pp. 68–71, 2019.
[20] M. H. M. Shamim, T. K. Ng, B. S. Ooi, and M. Z. M. Khan, "Tunable self-injection locked green laser diode," *Opt. Lett.*, vol. 43, no. 20, pp. 4931–4934, 2018.
[21] M. H. M. Shamim *et al.*, "Investigation of self-injection locked visible laser diodes for high bit-rate visible light communication," *IEEE Photon. J.*, vol. 10, no. 4, Aug. 2018, Art. no. 7905611.
[22] M. H. M. Shamim *et al.*, "Analysis of optical injection on red and blue laser diodes for high bit-rate visible light communication," *Opt. Commun.*, vol. 449, pp. 79–85, 2019.
[23] M. de Labachelerie, H. Sasada, and G. Passedat, "Mode-hop suppression of Littrow grating-tuned lasers: Erratum," *Appl. Opt.*, vol. 33, no. 18, pp. 3817–3819, 1994.
[24] New Focus: Tunable Lasers Brochure, Newport company, Santa Class, Ca 95054, USA. [Online]. Available: https://www.newport.com/medias/sys_master/images/images/h3d/h9b/8797219749918/New-Focus-Tunable-Diode-Lasers-Brochure.pdf.
[25] P. Mahnke, H. H. Klingenberg, and W. Zirnig, "Fast tuning of external-cavity diode lasers," *Appl. Opt.*, vol. 41, no. 30, pp. 6380–6384, 2002.
[26] C. J. Hawthorn, K. P. Weber, and R. E. Scholten, "Littrow configuration tunable external cavity diode laser with fixed direction output beam," *Rev. Sci. Instrum.*, vol. 72, no. 12, pp. 4477–4479, 2001.
[27] J. Ohtsubo, *Semiconductor Lasers*, 4th ed. Cham, Switzerland: Springer International Publishing AG 2017, 2013.